Radiological Physics and Technology (2018) 11:184–191
https://doi.org/10.1007/s12194-018-0454-5

Dosimetric changes with computed tomography automatic tube-current modulation techniques

Sofia Spampinato[1,2,4] · Anna Maria Gueli[1,2] · Pietro Milone[2,3] · Luigi Angelo Raffaele[1,2,3]

Received: 25 August 2017 / Revised: 24 March 2018 / Accepted: 27 March 2018 / Published online: 6 April 2018

Abstract
The study is aimed at a verification of dose changes for a computed tomography automatic tube-current modulation (ATCM) technique. For this purpose, anthropomorphic phantom and Gafchromic® XR-QA2 films were used. Radiochromic films were cut according to the shape of two thorax regions. The ATCM algorithm is based on noise index (NI) and three exam protocols with different NI were chosen, of which one was a reference. Results were compared with dose values displayed by the console and with Poisson statistics. The information obtained with radiochromic films has been normalized with respect to the NI reference value to compare dose percentage variations. Results showed that, on average, the information reported by the CT console and calculated values coincide with measurements. The study allowed verification of the dose information reported by the CT console for an ATCM technique. Although this evaluation represents an estimate, the method can be a starting point for further studies.

Keywords Noise index · Radiochromic films · CTDI · DLP · Anthropomorphic phantom

1 Introduction

Until the early 2000s, whole-body computed tomography (CT) scanners required manual selection parameters such as tube potential, tube current, rotation time, and pitch. Recognizing that the *automatic-exposure control* (AEC) features used in radiography could play an important role in CT technology, manufacturers developed specific CT AEC techniques.

In general, AEC applies to two aspects of parameter selection: *overall exposure control* and *tube-current modulation*. Overall exposure control increases the overall dose levels for larger patients and decreases the dose levels for smaller patients to obtain a comparable image quality. To penetrate larger patients and thicker body parts, the incident X-ray beam intensity needs to be increased to reach the detectors. On the other hand, for smaller patients, the X-ray beam intensity can be decreased and dose levels can thus be reduced [1].

Automatic Tube-Current Modulation (ATCM) techniques enable automatic adjustment of the tube current in the *x*–*y* plane (*angular modulation*, Fig. 1a) or along the *z*-axis (*longitudinal modulation*, Fig. 1b) according to the size and to the attenuation characteristics of the body part being scanned and to achieve a comparable image quality in all slices acquired. The combination of the two techniques allows three-dimensional current modulation (3D-ATCM) [2]. Unfortunately, owing to rapid technologic advances, vendors have developed ATCM techniques that use slightly different metrics to assess image quality and proprietary nomenclature [3]. Some manufacturers employ

✉ Sofia Spampinato
sofia.spampinato@ct.infn.it; sofspa@rm.dk

1 PH3DRA Laboratories (PHysics for Dating Diagnostic Dosimetry Research and Applications), Dipartimento di Fisica e Astronomia, Università di Catania and INFN-Catania, Via Santa Sofia 64, 95123 Catania, Italy

2 Scuola di Specializzazione in Fisica Medica, Dipartimento di Scienze mediche chirurgiche e tecnologie avanzate "G. F. Ingrassia", Scuola Facoltà di Medicina, Via Santa Sofia 78, 95123 Catania, Italy

3 Unità Operativa Complessa di Radiodiagnostica e Radioterapia, Azienda Ospedaliero-Universitaria Policlinico di Catania, P. O. Gaspare Rodolico, Via Santa Sofia 78, 95123 Catania, Italy

4 Department of Oncology, Aarhus University Hospital, Nørrebrogade 44, 8000 Aarhus, Denmark

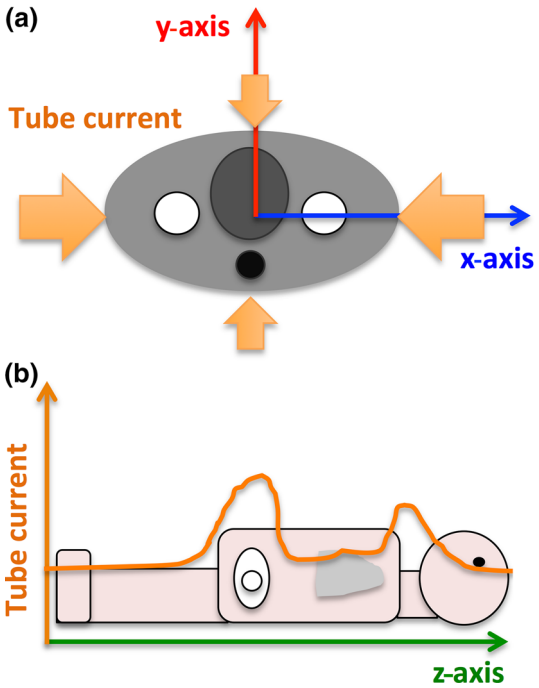

Fig. 1 Angular (**a**) and longitudinal (**b**) tube-current modulation

a simple measure of image noise, while others use a measure related to a reference image that accepts higher noise levels in more attenuating parts with higher contrast. However, the main principle is to manage image quality and radiation dose by adapting the tube current to the shape, size, and attenuation of the patient [4, 5].

Several studies have presented the variation in patient dose with patient size under ATCM operation [6–9] and the optimization of image noise and dose as a function of patient size [10, 11]. Most of the studies reference to the variation of volume CT dose index ($CTDI_{vol}$) (or dose–length product, DLP), the standard index for dosimetry in CT, which is currently displayed at the time of selection of the parameters, before a clinical CT examination. However, $CTDI_{vol}$ and DLP have recently been called into question, as they do not take into account the significant technological advances in CT, including ATCM techniques.

Based on these remarks, the proposed work is aimed at two objectives: (1) to verify that the $CTDI_{vol}$ and the DLP values reported by the CT scanner console actually reflect the dose distribution within the patient using radiochromic films and an anthropomorphic phantom and (2) to verify that the results coincide with the requirements of the quantum noise theory on which the ATCM technique is based.

2 Materials and methods

Our study focused on the ATCM technique developed by GE Healthcare (Milwaukee, WI., USA). This technique provides longitudinal AEC (AutomA) and angular AEC (SmartmA). Based on each patient's attenuation values measured from the scan projection radiograph (SPR), the tube current is adjusted to preserve the same noise level in each image on the *x*–*y*–*z*-axis [12].

For the purposes of this study, Gafchromic® XR-QA2 films, two-dimensional dosimeters that change color when exposed to ionizing radiation and an anthropomorphic phantom were used. Other studies with similar experimental setup and with satisfactory results are reported in the literature [14, 15].

2.1 Automatic-exposure control mechanism and quantum noise theory

The GE ATCM technique aims to maintain the image quality throughout the scan using the *noise index* (NI) parameter. Based on attenuation values for each patient measured from the SPR, the tube current is adjusted to preserve the same noise level on each slice. Changing NI modifies the range of milliampere over which the ATCM varies during each gantry rotation [4].

The AutomA module uses a single SPR for determining patient size, anatomic shape and attenuation characteristics to adjust tube current along *z*-axis. The SmartmA module, adjusts the tube current for different projection angles within each X-ray tube rotation. For each rotation (4 times/turn), the system calculates each *x* and *y* current value *in* mA from the relation between the long and short axes of the patient, based on the SPR image.

To use AutomA, SmartmA, and their combination, the operator must specify an NI value and current (mA) range in terms of a minimum and maximum tube-current value. These limits define the current modulation range.

The NI parameter allows an operator-desired image quality to be set, and it is referenced to the image noise, i.e., the standard deviation (SD) expressed in Hounsfield units (HU) of a region-of-interest (ROI) in the central region of the image of a uniform phantom with the patient's attenuation characteristics. The algorithm preserves the same image noise level as the attenuation values change from one rotation to the next [12].

The NI can be expressed in HU, because it approximates the SD in HU on CT images of a phantom. However, the SD in a real image is sometimes different from the operator selected NI. NI, in fact, adjusts the tube current (i.e., quantum noise), but image noise depends also on other factors such as electronic noise, patient characteristics, tube

voltage, filtration, reconstruction filter, slice thickness pitch, and matrix dimensions [16].

The NI, based on Poisson statistics, is proportional to the inverse dose (D) square root. Thus, as NI is decreased to reduce the noise, the radiation dose must increase. Related to the number of X-ray photons per voxel, N, the following relation for the SD of the photon count measured, σ, is valid:

$$\sigma = \sqrt{N}.$$

The *relative noise*, measured on the CT scanner console in an ROI of the image, is defined by

$$\frac{\sigma}{N} \propto \frac{1}{\sqrt{N}} = NI \propto \frac{1}{\sqrt{D}}.$$

Each examination protocol is performed using a reference image noise index (NI_{ref}) value recommended by the manufacturer. This image noise index may be modified by the CT operator if images at a lower or a higher noise, compared to the reference, are desired. This NI modification alters the patient radiation dose. To calculate the dose difference (ΔD) between acquisitions performed using NI_{ref} and the modified noise index (NI_{ε}), the following equation may be used:

$$\frac{\Delta D}{D} = \frac{1-(1+\varepsilon)^2}{(1+\varepsilon)^2}, \quad (1)$$

where ε is defined as [16]

$$\varepsilon = \frac{NI_{\varepsilon} - NI_{ref}}{NI_{ref}}.$$

Using the expression (1), it is possible to make a preliminary calculation the percentage dose change resulting from the difference between an NI value and a reference NI value. A significant increase of image noise might not necessarily worsen the overall image quality while allowing, however, a decrease in the total delivered dose. On the other hand, a slight improvement of image quality may not significantly increase the clinical information content, resulting, however, in an unnecessary dose increase. Equation (1) will be used to calculate the predicted dose variations obtained by modifying the NI.

2.2 GafChromic® XR-QA2 film calibration and processing

The GafChromic® XR-QA2 series is optimized for radiology energies (20–200 kVp) and doses (0.1–20 cGy) and is designed as a tool for quality assurance [13]. The characterization of the film, which is beyond the scope of this work, has been duly performed as reported in the previous studies [17–20]. In particular, it has been verified that the dose dependence (e.g., from the tube current) of the film response is not influential, introducing an uncertainty of less than 0.5%. With regard to the angular dependence of the film response, some studies have verified that it can introduce significant uncertainties in particular configurations [21, 22]. However, it has been verified that a complete scan, which corresponds to the real irradiation conditions in CT, introduces overall uncertainty of 2% [21]. In addition, experimental maps were normalized with respect to the reference dose map, thus obtaining dose variations relative to the reference noise value.

For calibration, 3 cm × 3 cm film samples were irradiated at increasing air kerma values from 1 to 150 mGy using a conventional X-ray tube, reproducing an effective energy value near to that used in CT to minimize the error due to film energy dependence.

Twenty-four hours after radiation exposure, the films were digitized with a commercial optical scanner (Epson Expression 10000XL). This procedure allowed us to obtain images in which the air kerma calibration was applied for post-processing [17–19, 23].

2.3 Anthropomorphic phantom study

For the purposes of this study, a male Alderson Rando (AR) phantom was used. The AR phantom, composed of tissue-equivalent material, represents an adult with a height of 175 cm and weight of 73.5 kg, and is transected horizontally into 2.5 cm-thick slices. This configuration makes it suitable for insertion of radiochromic films between slabs [24].

Radiochromic films were cut to the shape of two slabs of the AR phantom in two different anatomical regions (shoulders and mid-thorax). The choice was based on different tissue compositions, respectively, higher bone content and higher lung content.

ATCM is available with the CT scanner used for the measurements reported here (GE Optima CT660). The modulation algorithm is based on the antero-posterior (AP) SPR of the patient. It has been shown that an AP SPR ensures the lowest dose levels [25]. A thorax acquisition protocol was selected, as it represents one of the most important applications of ATCM techniques.

To select the NI values to be used, a preliminary study was carried out with a senior radiologist to visually analyze image quality by varying the NI. In this way, three important values of NI with comparable image quality were identified: 13 (recommended by the manufacturer), 10 (lower noise), and 16 (higher noise). For these three values of NI, a quantitative evaluation of image quality was performed on different ROIs in different positions within the phantom. The image quality evaluation was performed by analyzing median and SD values (expressed in HU) of ten ROIs, each of an area of 1 cm^2, in different sections of the

phantom, from the shoulders to the mid-thorax; ROIs were placed in areas of soft tissue, lungs, and near bony interfaces. The positions of the ten ROIs were the same for the three (NI = 10, 13, and 16) different scans, guaranteeing meaningful comparisons of SD and median values. All the CT acquisition parameters, with the exception of the NI, were kept constant. The scans were performed in helical mode with a pitch of 0.984, voltage of 120 kV, collimation of 40 mm, Scan Field Of View (SFOV) Large Body, and a rotation time of 0.6 s. The minimum and maximum current values were set as 100 and 400 mA, respectively. A total of six films were irradiated: three UP (shoulder region) and three DOWN (mid-thorax region), as shown in Fig. 2.

The CT scanner console shows before an exam, and in the final DICOM (Digital Imaging and Communications in Medicine) Dose Report, the CTDIvol and DLP values calculated on the basis of the acquisition parameters. These values allow comparisons of dose variations between values calculated theoretically using ε and values measured experimentally with the AR phantom and radiochromic films.

The irradiated films were digitized with flatbed scanner using the following acquisition parameters: resolution of 72 dpi, color depth of 48 bit, TIFF format, and all color and correction filters turned off. The image processing and calibration was performed with the open source software ImageJ 1.49n (National Institutes of Health, Bethesda, MD). The data analyses were performed with Origin 8 (OriginLab Corporation, Northampton, MA). The dose matrices obtained for NI equal, respectively, to 10 and 16 were normalized with respect to the NI_{ref} dose matrix (13).

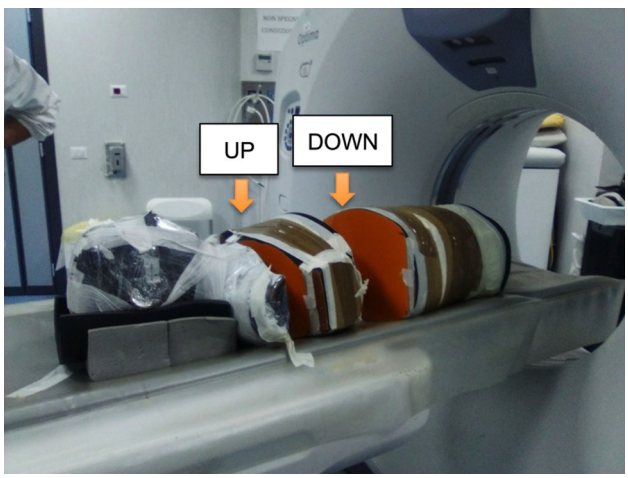

Fig. 2 Experimental setup for the AR phantom irradiation

3 Results

The results of the quantitative study of image quality and the theoretical–experimental comparison of dose are presented below.

3.1 Image quality evaluation

Table 1 shows median values obtained in the three scans and the differences calculated with respect to the reference values (NI = 13). Median values are indicative of the location of ROI (soft tissue, lungs, or bony regions). For some ROIs, in fact, the correspondence between NI and SD is valid, while for others, this does not occur. This could be influenced by the composition of the analyzed tissue: if composition is "similar" to water, the correspondence between NI and SD should be more valid.

The median values and the range of the differences between the standard deviations, which in the presence only of quantum noise should correspond to NI, are 2.3 [0.1–4.8] and − 3.1 [− 5.5 to + 6.1] for NI = 10 and NI = 16, respectively. Though the median values correspond to the difference in NI, the range of values is wide and confirms the presence of other factors contributing to noise. It is interesting to note that, especially in the case of the image ROI of the lungs, the median value correspondence with the NI difference no longer holds.

3.2 Experimental results

Table 2 shows $CTDI_{vol}$ and DLP values reported by the CT scanner console for the selected NI values, keeping constant all other acquisition parameters. The percentage changes were calculated with respect to NI_{ref}. Improving image quality (NI = 10), the dose reported by the CT scanner console increases by 63%. Similarly, increasing image noise (NI = 16), the dose decreases by about 40%.

Figure 3 shows false color contour plots of experimentally measured dose relating to (1) NI = 10 and (2) NI = 16 normalized to the NI = 13 dose matrix. The color scales are from 0 to 250 for NI = 10 and from 0 to 150 for NI = 16. This choice allows better appreciation of the differences, both positive and negative, in the two cases. For NI = 10, higher doses are present at the mid chest (marked DOWN in Fig. 3), with differences hot spots of 200%, particularly at the surface of the AR phantom.

On average, for NI = 10, the dose increases approximately 50–60% for the shoulder region (UP) and 50–70% for the mid-chest region (DOWN). Similarly, for NI = 16, reductions of 30–40% of the dose for the shoulder region (UP) and of 25–35% for the mid-chest region (DOWN) are present. Therefore, the analysis allows us to deduce that the

Table 1 Median values and standard deviations measured in 10 different ROIs within the phantom for the reference NI (13), decreasing noise (10) and increasing noise (16)

ROI #	NI = 13 (ref)		NI = 10				NI = 16			
	Median	SD	Median	Difference median	SD	Difference SD	Median	Difference median	SD	Difference SD
1	11.9	14.2	10.7	1.2	11.8	2.4	11.1	0.8	19.7	− 5.5
2	5.2	18.5	4.0	1.2	13.7	4.8	9.8	− 4.6	21.6	− 3.1
3	11.5	14.5	9.3	2.2	11.5	3.0	10.1	1.4	17.5	− 3.0
4	3.3	12.0	4.8	1.5	8.9	3.1	3.0	0.3	14.1	− 2.1
5	− 0.9	13.3	3.6	4.5	11.1	2.2	2.2	− 3.1	17.4	− 4.1
6	− 704.1	14.4	− 707.5	3.4	13	1.4	− 706.4	2.3	16.6	− 2.2
7	− 8.5	10.9	1.0	9.5	9.5	1.4	− 3.2	− 5.3	13.9	− 3.0
8	− 662.9	4.5	− 658.9	4.0	44.4	0.1	− 669.9	7.0	38.4	6.1
9	1.9	12.1	3.3	1.4	10.5	1.6	2.9	− 1.0	15.7	− 3.6
10	16.1	12.2	12.1	4.0	8.8	3.4	14.8	1.3	16.6	− 4.4

All values and differences are expressed in HU

Table 2 $CTDI_{vol}$ and the DLP values reported by the CT scanner console

NI	$CTDI_{vol}$ (mGy)	DLP (mGy cm)	% Difference
13	11.26	420.61	–
10	18.47	689.93	+ 64
16	7.72	288.38	− 32

Percentage variation calculation compared to the reference (NI = 13) is required for the other comparisons

ATCM performance is more effective for the shoulder region (UP), since it permits a more efficient decrease the dose, moving NI upwards compared to reference, while moderating the dose increase as NI moves in the opposite direction compared to the reference.

3.3 Theoretical and experimental comparison

Using Eq. (1), it is possible to calculate the percentage dose variations due to NI variation from NI_{ref}. Increasing the quantum noise, thereby increasing NI to 16, the corresponding ε value is + 0.23. Substituting this value in the expression (1), the dose decrease is 35%. On the other hand, decreasing the quantum noise and changing NI to 10, the ε value is –0.23, and the corresponding dose increase is 70%.

Although the modulation current effect should ensure a consistent image quality throughout the entire scan, the dose distribution is not uniform within the patient, as simulated by the AR phantom. This study is limited by the analysis of only two individual sections, which, however, correspond to two significant regions in the thorax. Table 3 summarizes the results obtained in the three cases: theoretical, experimental, and those reported from the CT scanner console.

4 Discussion

Automatic-exposure control (AEC) techniques reduce the radiation dose to the patient based on their physical dimensions and tissue absorption properties. The use of ATCM techniques is already common in CT imaging of the torso, as well as in the head and neck regions, thus allowing a considerable reduction of the dose to the patient [2, 3, 6–8, 10, 11].

Dosimetry in CT is still a complex issue. The standard reference indices are $CTDI_{vol}$ and DLP metrics, reported before and at the end of an exam in a DICOM Dose Report. However, these two parameters have recently been called into question. First, they do not take into account significant technological advances, including ATCM techniques. Moreover, these metrics do not consider the actual patient's size, but only scanner output parameters [26]. The Association of American Medical Physics (AAPM) has introduced the Size-Specific Dose Estimate (SSDE), a new index that represents a more realistic dose estimate [27, 28].

However, when ATCM techniques are used, the assessment of the SSDE is not very straightforward. A more accurate estimate can be achieved if a slice-by-slice evaluation of the constant water-equivalent patient diameter is made and the tube current–time product for each CT image is known. [1]. The application of this procedure is

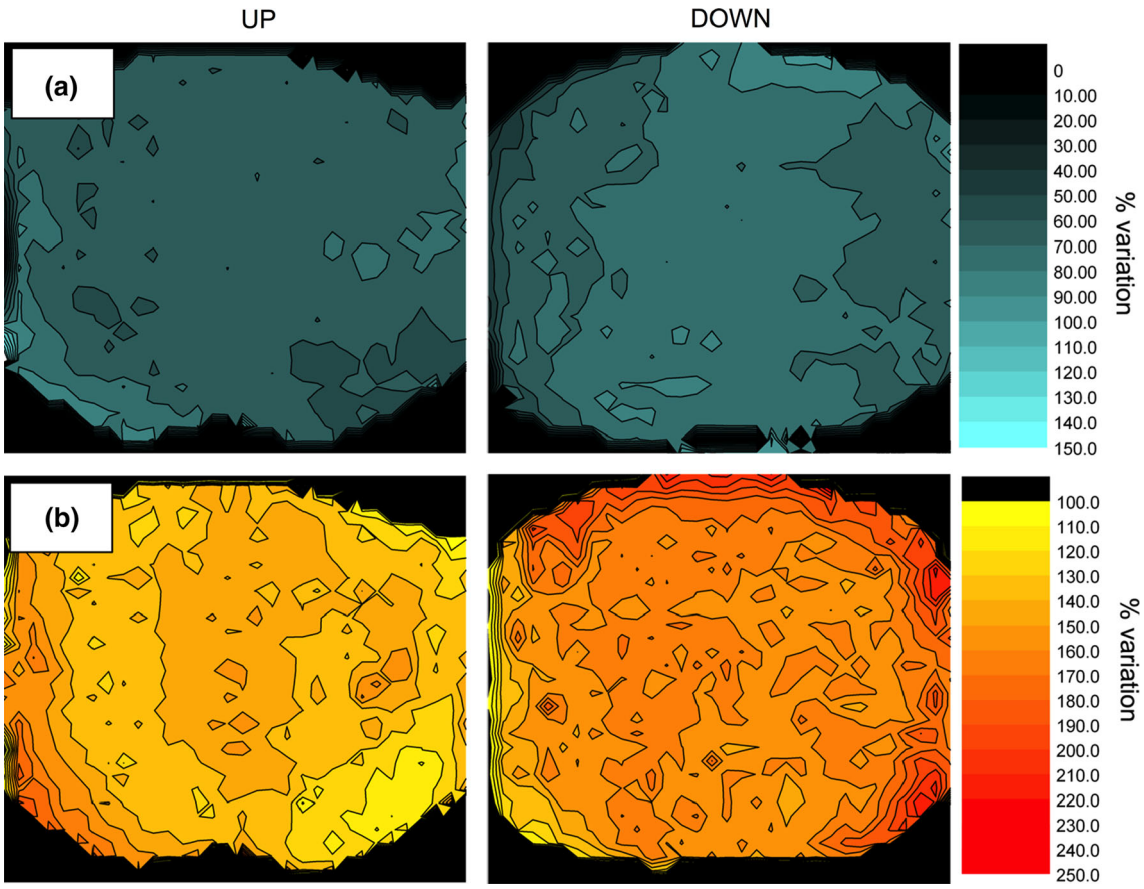

Fig. 3 Measured experimental dose maps, normalized to the reference NI value (NI = 13) relating to **a** NI = 10 and **b** NI = 16 for two sections, shoulders (UP) and the chest (DOWN)

Table 3 Results of dose variation derived from Poisson statistics (theoretical), relative variation of the dosimetric indices reported from the console ($CTDI_{vol}$ and DLP), and average measured dose variation for two sections: shoulders (UP) and the chest (DOWN)

Dose variation					
NI	Theoretical (%)	Console (%)		Experimental (%)	
16	− 40	$CTDI_{vol}$	− 32	Up	− 30 to 40
		DLP		Down	− 25 to 35
10	+ 70	$CTDI_{vol}$	+ 64	Up	+ 50 to 60
		DLP		Down	+ 60 to 70

not simple, and dose comparisons on the basis of this index are not yet widespread.

Several studies have evaluated dose variations using different ATCM techniques in terms of $CTDI_{vol}$ and DLP, proving a certain benefit for patient dose sparing [4, 15, 29]. Since these metrics are not entirely representative of the current absorbed dose, it is interesting to evaluate how the CT scanner console predictions are verified within the patient in terms of real dose distribution.

Based on these observations, the present work aimed to evaluate experimentally dose variations in an anthropomorphic phantom using the GE Healthcare ATCM technique. The parameter related to image quality is the Noise Index, representative of the quantum noise, which can be varied to improve or worsen the image quality. The study had two particular objectives that are to verify that measured dose changes correspond to those (1) calculated with Poisson statistics underlying the NI theory and (2) provided by the CT scanner before the examination in terms of $CTDI_{vol}$ and DLP.

For this purpose, Gafchromic XR-QA2 radiochromic films were used. The main advantage is the possibility of acquiring dose maps with high spatial resolution. In addition, radiochromic films can be easily inserted into an anthropomorphic phantom without perturbing the system. Other authors have used similar setups for dose evaluations in CT, obtaining satisfactory results. [14, 15].

Starting from a reference protocol (recommended by the manufacturer) with an NI equal to 13 (NI_{ref}), the image noise was decreased (NI = 10) and increased (NI = 16) so as not to affect significantly the image quality. Quantitative study on the image quality allowed us to verify that the SD

measured in different ROIs within the phantom does not always correspond to the NI provided by the scanner, testifying that quantum noise is not the only noise component contributing to noise in the CT image.

The values obtained by Poisson statistics can be compared with the dosimetric data reported by the CT scanner console before the examination.

Table 3 shows $CTDI_{vol}$ and the DLP values for the selected NI values, keeping constant all other acquisition parameters. The percentage changes were calculated with respect to NI_{ref}. Improving image quality (NI = 10), the dose reported by the CT scanner console increases by 63%. Similarly, increasing image noise (NI = 16), the dose decreases by about 40%.

The values reported by the CT scanner console are in agreement with values previously calculated using Poisson statistics. Although the result was expected, the comparison is a validation of the correct operation of the ATCM algorithm. The values reported by the CT scanner console are, in fact, developed from $CTDI_{vol}$ values measured with the standard procedures. Comparing these results with measurements performed with the AR phantom, the agreement is good and confirms the reported data both theoretically and from the CT scanner console. Excluding some hot spots and colder regions, the agreement is valid on average by 10%. However, as previously mentioned, the distribution is not uniform in all sections and the increase or decrease of the dose is not the same everywhere. In particular, the modulation algorithm seems more effective for shoulders than for mid-thorax, where it always recorded a higher dose. However, the overall estimate provided by the CT scanner console and the DICOM Dose Report at the end of the examination is on average a good approximation of dose variations due to an appropriate choice of NI. The protocol optimization, which is not covered by this study, strongly depends on the particular ATCM technique used and on operator choices. Literature provides some tips for good development of ATCM systems [5], but at present, there is not a standard method and the optimization is entrusted to the experience of the operator.

The main limitation of the study was the lack of analysis of dose distribution in the absence of tube-current modulation. This measurement would have shown the advantages of using this technique in clinical practice. Furthermore, this study is also limited to the analysis of two anatomical sections, and therefore, it does not give a complete overview. However, the results may represent a starting point for future studies regarding this topic and, in general, to dose distribution analysis in CT. In general, the methodology proposed is applicable to any ATCM technique, correlating dose variations provided by the CT scanner with experimental values. Radiochromic films, moreover, allow the creation of high-resolution dose maps more easily than other detectors (i.e., thermoluminescence or optically stimulated luminescence dosimeters), and are suitable for dose measurements in anthropomorphic phantoms.

5 Conclusions

Dosimetry in CT is currently based on indices ($CTDI_{vol}$ and DLP) which do not take into account the size of the patient or consider new technological developments such as ATCM techniques. The study enabled us to verify that the percentage variations of $CTDI_{vol}$ and DLP reported by the CT scanner console after an examination with ATCM techniques, as well as the theoretical values calculated according to quantum noise theory, correspond to variations measured experimentally with the use of an anthropomorphic phantom and radiochromic films. Further studies may be conducted to obtain information on absorbed doses to individual organs using ATCM or organ effective modulation (OEM) techniques to assess their actual benefits.

Compliance with ethical standards

Conflict of interest The authors declare that they have no conflict of interest.

Statement of human rights This article does not contain any studies with human participants performed.

Statement of animal rights This article does not contain any studies with animals performed.

Informed consent Informed consent was obtained from all individual participants included in the study.

References

1. International Commission on Radiation Units and Measurements. ICRU report no. 87: radiation dose and image-quality assessment in computed tomography. J ICRU. 2012;12(1):1–149.
2. Lee CH, Goo JM, Lee HL, Ye SJ, Park CM, Chun EJ, Im JG. Radiation dose modulation techniques in the multidetector CT era: from basics to practice. RadioGraphics. 2008;28:1451–9.
3. Kalra MK, Maher MM, Toth TL, Schmidt B, Westerman BL, Morgan HT, Saini S. Techniques and applications of automatic tube current modulation for CT. Radiology. 2004;233(3):649–57.
4. Söderberg M, Gunnarsson M. Automatic exposure control in computed tomography—an evaluation of systems from different manufacturers. Acta Radiol. 2010;51(6):625–34.
5. Martin CJ, Sookpeng S. Setting up computed tomography automatic tube current modulation systems. J Radiol Prot. 2016;36(3):R74–95.
6. Schindera ST, Nelson RC, Toth TL, Nguyen GT, Toncheva GI, DeLong DM, Yoshizumi TT. Effect of patient size on radiation

dose for abdominal MDCT with automatic tube current modulation: phantom study. Am J Roentgenol. 2008;190(2):W100–5.
7. Israel GM, Cicchiello L, Brink J, Huda W. Patient size and radiation exposure in thoracic, pelvic, and abdominal CT examinations performed with automatic exposure control. AJR. 2010;195:1342–6.
8. Meeson S, Alvey CM, Golding SJ. The in vivo relationship between cross-sectional area and CT dose index in abdominal multidetector CT with automatic exposure control. J Radiol Prot. 2010;30(2):139–47.
9. Sookpeng S, Martin CJ, Gentle D. Comparison of different phantom designs for CT scanner automatic tube current modulation system tests. J Radiol Prot. 2013;33(4):735–61.
10. Siegel MJ, Schmidt B, Bradley D, Suess C, Hildebolt C. Radiation dose and image quality in pediatric CT: effect of technical factors and phantom size and shape. Radiology. 2004;233(2):515–22.
11. Verdun FR, Lepori D, Monnin P, Valley JF, Schnyder P, Gudinchet F. Management of patient dose and image noise in routine pediatric CT abdominal examinations. Eur Radiol. 2004;14(5):835–41.
12. http://www3.gehealthcare.co.uk. Accessed 6 Apr 2018.
13. http://www.gafchromic.com. Accessed 6 Apr 2018.
14. Brady S, Yoshizumi T, Toncheva G, Frus D. Implementation of radiochromic film dosimetry protocol for volumetric dose assessments to various organs during diagnostic CT procedures. Med Phys. 2010;37(9):4782–92.
15. Sookpeng S, Butdee C. Signal-to-noise ratio and dose to the lens of the eye for computed tomography examination of the brain using an automatic tube current modulation system. Emerg Radiol. 2017;24(3):233–9.
16. Kanal KM, Stewart BK, Kolokythas O, Shuman WP. Impact of operator-selected image noise index and reconstruction slice thickness on patient radiation dose in 64-MDCT. AJR. 2007;189:219–25.
17. Spampinato S (2016) Radiochromic film dosimetry in computed tomography. Unpublished thesis, Specialization School in Medical Physics, Università di Catania, Catania, Italy.
18. Rampado O, Garelli E, Deagostini S, Ropolo R. Dose and energy dependence of response of Gafchromic XR-QA film for kilovoltage X-ray beams. Phys Med Biol. 2006;51:2871–81.
19. Tomic N, Quintero C, Whiting BR, Aldelaijan S, Bekerat H, Liang L, DeBlois F, Seuntjens J, Devic S. Characterization of calibration curves and energy dependence GafChromic^{TM} XR-QA2 model based radiochromic film dosimetry system. Med Phys. 2014;41(6):062105-1–9.
20. Di Lillo F, Mettivier G, Sarno A, Tromba G, Tomic N, Devic S, Russo P. Energy dependent calibration of XR-QA2 radiochromic film with monochromatic and polychromatic X-ray beam. Med Phys. 2016;43:583–8.
21. Rampado O, Garelli E, Ropolo R. Computed tomography dose measurements with radiochromic films and a flatbed scanner. Med Phys. 2010;37(1):189–96.
22. Giaddui T, Cui Y, Galvin J, Yu Y, Xiao Y. Characteristics of Gafchromic XRQA2 films for kV image dose measurement. Med Phys. 2012;39(2):842–50.
23. Asero G, Greco C, Gueli AM, Raffaele L, Spampinato S. Evaluation of spatial resolution in image acquisition by optical flatbed scanners for radiochromic film dosimetry. JINST. 2016;11:P03024.
24. http://www.rsdphantoms.com/rt_art.htm. Accessed 6 Apr 2018.
25. Moro L, Panizza D, D'Ambrosio D, Carne I. Considerations on an automatic computed tomography tube current modulation system. Radiat Prot Dosim. 2013;156(4):525–30.
26. Huda W, Mettler FA. Volume CT dose index and dose-length product displayed during CT: what good are they? Radiology. 2011;258(1):236–42.
27. American Association of Physicists in Medicine (2011) Size-specific dose estimates in pediatric and adult body CT examinations. AAPM report no. 204. ISBN: 978-1-936366-08-8.
28. American Association of Physicists in Medicine (2014) Use of water equivalent diameter for calculating patient size and size-specific dose estimates (SSDE) in CT. AAPM report no. 220. ISBN: 978-1-936366-39-2.
29. McCollough CH, Bruesewitz MR, Kofler JM Jr. CT dose reduction and dose management tools: overview of available options. Radiographics. 2006;26:503–12.